



Comparative Analysis of CNN Architectures for Classification of Breast Histopathological Images

Aditi Kajala¹, Sandeep Jaiswal² and Rajesh Kumar³

¹ Computer Science & Engineering , Mody University of Science & Technology, Lakshmanagarh, India

² Biomedical Engineering , Mody University of Science & Technology, Lakshmanagarh, India

³ Electrical Engineering , Malaviya National Institute of Technology , Jaipur, India

E-mail: aditikajala@gmail.com

Article History: Received: 22.05.2023

Revised:20.06.2023

Accepted: 03.07.2023

Abstract

Breast cancer is one of the leading causes of cancer death in women all over the world. The emergence of digital imaging and computational aids in medicine has improved the diagnostic accuracy of breast cancer and reduced the workload of pathologists. Convolutional Neural Networks (CNNs) have recently emerged as a favored deep learning technique for breast cancer detection and classification.

This paper presents a comparison of various deep convolutional neural networks (CNN), EfficientNet architectures (B1-B7), VGG19, ResNet50, DenseNet169, and InceptionV3 architectures for the classification of histopathology images of breast cancer. All architectures are tested on a publicly accessible histopathology image dataset. To minimize overfitting, data augmentation techniques are also used during training CNN models. According to the findings of the investigation, the EfficientNet-B6 model had a validation accuracy of 96.9% and a validation loss of 0.0898 in comparison to other tested models.

Keywords: Breast Cancer, CNN, EfficientNet, Compound scaling, Data augmentation, Histopathology Images

1. Introduction

Breast cancer is the most prevalent tumor and a common cause of death in women in India as well as all over the world. [1-2]. Published report GLOBOCAN2020 showed that female breast cancer has surpassed lung cancer with 2.3 million new cases (11.7 %) worldwide [2]. The number of cancer cases [3] in India is estimated to be 15.7 lakh by 2025. National Cancer Registry Program Report [4] also estimated that women's breast cancer is going to contribute 14.8 % of overall cancer cases by the year 2025. Breast cancer has a significant impact not only on a woman's physical health, but also on her mental and emotional well-being. As a result, it is important to address it.

To diagnose breast cancer surgical biopsy techniques are commonly used in pathologies [5]. To diagnose and investigate the malignancy in the tissues from the biopsy histopathology examination under a microscope is done by a pathologist. The degree of experience of the pathologists engaged in the analysis may have an impact on the results [5]. The detection of breast cancer at early-stage can reduce the mortality rate due to the disease [6-7]. Therefore it is the need of time to find an efficient, accurate method to diagnose malignancies in breast at early stages with minimum human intervention.

Traditional machine learning algorithms [8-9] worked using hand-crafted features or filters (Fig. 1) designed by a domain expert. Deep learning models have recently achieved significant advances in computer vision, particularly in medical image processing, because of their ability to learn complex tasks autonomously. Deep learning algorithms can assist doctors and specialists by providing a second opinion [12].

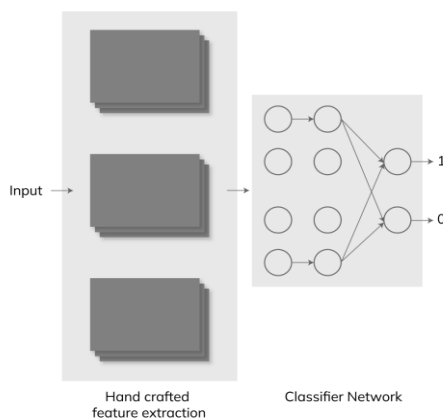


Fig. 1:Hand-crafted feature extractor(s) with traditional Machine Learning algorithm as classifier

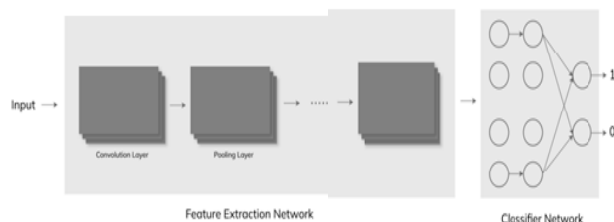


Fig. 2: Using deep learning algorithm as feature extractor network combined with traditional Machine Learning algorithm as classifier

Deep Learning algorithms such as CNN extracts complex information or hidden features from images, and then uses some classifier network (Fig. 2.) for classification. Therefore CNN can be used for feature extraction [10] also. By adding a series of convolutional, pooling layer a fully connected and classification layers (Fig. 3) CNN can also be used for classifying the images.

The main goal of the paper is to compare the performance of EfficientNet architectures (B1-B7), the performance of state of art VGG19, ResNet50, DenseNet169, and InceptionV3 are also compared for the classification of breast histopathology images. The contribution of the research is to confirm the better performance of EfficientNet architecture (B1-B7) over other state of art in terms of fast speed of computation in spite of larger number of parameters with Histopathology Cancer Detection Data set for malignancy classification since these architectures were previously used in literature with different data sets for similar task. The paper is divided into four sections. Section 2 presents the previous work. The applied methods and techniques are explained in section 3. The results of the experiments are presented and discussed in Section 4. Section 5 explains the conclusion and future scope of the work.

2. Previous Work

In both rural and urban India, breast cancer is growing more frequent [2]. It is reported that in India, one woman dies from breast cancer for every two newly diagnosed women [5]. The chances of mortality from cancer are reduced if it is detected early [11],[1],[12]. A survey of the literature revealed that numerous attempts have been made to identify breast cancer using histological images [1], [8],[10] and computer-aided diagnostic techniques yield astonishing results[13]. Traditional machine algorithms [14], [15],[16] were used to analyze the data using feature extraction techniques and required human intervention to label the training data [17]. Deep learning algorithms on the other hand directly apply raw images and required less expert knowledge and effort to select many important features [11]. Deep learning methods work on the concept of revealing hidden patterns in the images and then using them in classifying into various classes [12]. The diagnostic capabilities of deep learning algorithms are competing the levels of human expertise [18]. The previous work of various researches using CNN architectures for breast cancer detection from histopathologic images are summarized in table I

2.1 CNN with Transfer Learning

InceptionV4 architecture and Residual connection were applied on the ICIAR-2018 dataset for Breast cancer classification histopathology images [8]. Transfer learning was applied to avoid training of the model from scratch. with a softmax activation function. The authors compared the accuracy of simple CNN, InceptionV4, and InceptionV4 with augmentation for patch-wise classification on training as well as on testing for the whole image classification and individual classes classification. To classify histopathology into Carcinoma and non-carcinoma, the model achieved an accuracy of 93.7%. DenseNet as a basic building block, Squeeze-and excitation (SENet) [19] as classification subnetwork was integrated for Breast Cancer classification with the Breast Cancer Histopathological (BreakHis) data set. Different combination of DenseNet, SENet, and classification subnetwork for PRR (Patient RecognitionRate) and IRR (Image Recognition Rate) of different magnification factors were compared.

One major challenge in the classification of the histopathologic images is the variation of color and artifact due to the background of the image. So removing background from the image can also improve the accuracy of the model. The authors[20] emphasized the removal of background from histopathology images to extract tissue regions using U-Net. The performance of the four computer vision models were compared. EfficientNetB3, ResNet-50, and DenseNet-121 were used to predict lymph node metastasis in breast cancer[21] with Rectified Patch Camelyon (RPCam) data set. The best performance was observed with EfficientNet-B3 which gave 97.3 % of test accuracy. EfficientNet architectures were used to classify breast cancer histology images provided by ICIAR2018 dataset [1]. EfficientNet-B0 to EfficientNet-B6 were trained using transfer learning and evaluated to classify images into four classes: normal, benign, in situ carcinoma,

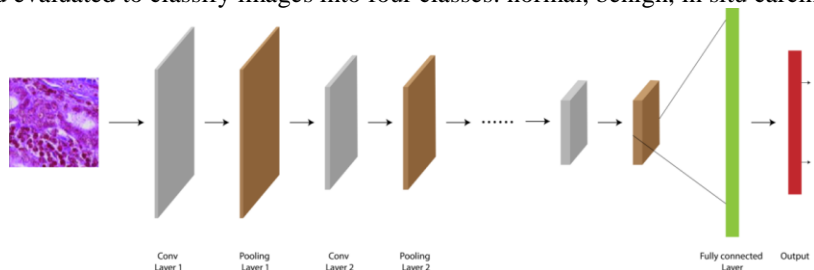


Fig.3: Using CNN as feature extractor and classifier

and invasive carcinoma. Reinhard and Macenko standard stain normalization techniques with EfficientNet architectures, were compared. The best performance was observed with EfficientNet-B2 which produced an accuracy of 98.33% using Reinhard stain normalization and 96.67% using Macenko stain normalization. The activation function used in various layers of CNN and optimizer also play important role in the classification problem[22]. 97.94% accuracy was achieved using Rectified Adam as optimizer and Mish as activation function with EfficientNet-B6 for binary classification with Patch-Camelyon(PCam) dataset.

Table I: Summary of previous researches for Breast cancer classification with transfer learning

Reference	Name of Architecture used or Architecture performed better	Dataset	Classification / Segmentation	Performance Metric
[8]	InceptionV4	ICIAR-2018	Binary	Accuracy :93.7%
[19]	DenseNet 121 with SENet	BeakHis	Binary	PRR:89.5, IRR:89.1
[20]	MobileNet And EfficientNet-B3	TCGA	Sementation	Sensitivity: 99%
[21]	EfficientNet-B3	RPCam	Binary	Accuracy: 97.9%
[22]	EfficientNet-B6	RPCam	Binary	Accuracy: 97.94%
[1]	EfficientNet-B2	ICIAR-2018	Multi class	Accuracy: 98.33%

2.2 Data Augmentation

The generalizability of the model is the difference between the performance of a model with training data (seen data) and test data (unseen data). A model can be made general by reducing overfitting. Overfitting can be reduced by applying drop-out layers, batch normalization, and L1/L2 regularization techniques[23]. Data augmentation[24] is the technique to increase the amount of data from existing data by applying some transformation keeping the labels preserved before training models. By augmentation diversity in data can also be increased. Diversity in data improves the performance of the models by reducing the overfitting issue. In the medical imaging domain, it is challenging to get a huge amount of labeled data. So data augmentation helps to increase the size of the data set. But it is also important to consider the safety of augmentation that preserves the label after augmentation. Some data augmentation techniques are as given as follows:

2.2.1 Geometric Transformation. These techniques are based on basic image manipulators like flip horizontally/vertically, affine (scaling, rotation, shear)[25]

2.2.2 Color Space Transformations. Images can be augmented by applying various blurring techniques. So changing the brightness of images can also increase the size of the data set. [26]

2.2.3 Noise Injections. Data can be augmented by introducing noise to the training data. There are various types of noise like additive noise, multiplicative noise, salt and pepper noise, and gaussian noise [27]

2.2.4 Advanced Data Augmentation. Data can also be augmented by adversarial training. In adversarial training, one model is used to classify the images and the other model adds noise to them. They both try to fool each other. Mixing the images generated through adversarial training in training dataset can also make models to learn more variety of features [28].

3. Methods and Techniques

Fig. 4 depicts the workflow of the experiment. The dataset was split into training and validation subsets named as 'Train', 'Val' respectively. The splitting of dataset was done with an 80:20 ratio. A customized image Data generator is used to apply the data augmentation to increase the size of the training dataset so that semantic information of the image would not be lost at the time of training the pre-trained model. The Val subset is also used to validate the model during training. After 20 epochs during the training phase, the Val subset is again supplied as input to the trained models, and the accuracy, precision, recall, and F-1 score of each model was computed.

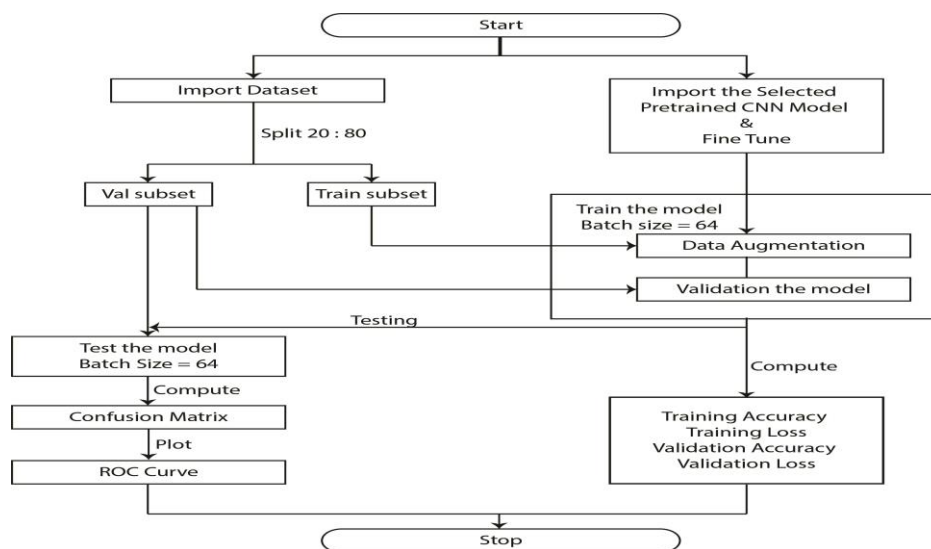


Fig.4. Work Flow of the approach

3.1 Data Set

Histopathology Cancer Detection dataset is available on Kaggle used for the presented study[29]. This dataset is a subset of the Patch-Camelyon [17] dataset. It consists of 400 H&E whole slide images of the sentinel lymph node section. These images were acquired and digitized at two centers using a 40x objective. There is a total of 220,025 images of benign and malignant(cancerous) classes. Fig.5. shows the distribution of both the classes in the dataset. It is shown that the data set consists 89117 cancerous and 130908 non-cancerous images. The images are in RGB and tiff format, with the size of 96x96 pixels. A cancerous image indicates that the patch contains at least one pixel from cancer tissue. For this binary classification problem the cancerous image is labelled with ‘1’ and non-cancerous image is labelled with ‘0’. Fig.6. depicts any random four labelled sample images from both classes of the data set.

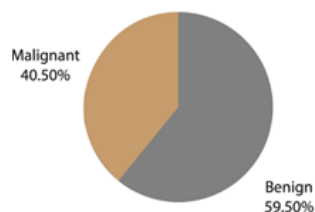


Fig.5. Distribution of images

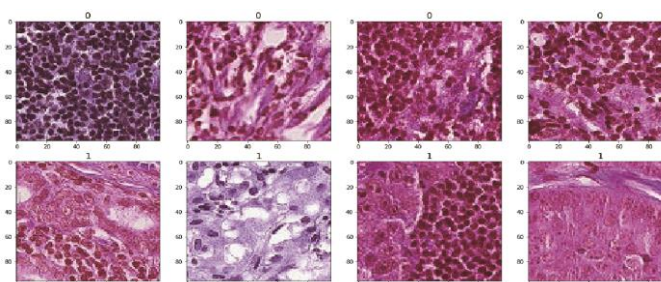


Fig.6. Sample tissue patterns shown in images of each class. [0:Benign, 1:Malignant]

3.2 Data augmentation

Data augmentation technique is applied through various augmenters available in imaug library[30]. Flipping, scaling, rotation, shearing and blurring are applied through various augmenters [31] from the library. Augmentation is applied only during training the model dynamically. So there is no need for additional storage.

3.3 EfficientNet Architectures

The family of EfficientNet CNN architectures consisting of eight architectures(B0-B7). These architectures work on the concept of compound scaling to increase the performance of pre-trained CNN models. Fig.7. depicts the difference between compound scaling and conventional scaling(in only unidirectional dimension for example width, depth, and resolution). A compound coefficient ϕ is used for scaling the network. Equation(1) represents the way of scaling the depth, width, and resolution with respect to ϕ [32]

$$\begin{aligned} \text{depth} : d &= \alpha^\phi, \\ \text{width} : w &= \beta^\phi, \\ \text{resolution} : r &= \gamma^\phi, \end{aligned} \quad (1)$$

$$\text{s.t } \alpha \cdot \beta^2 \cdot \gamma^2 \approx 2, \quad (2)$$

$$\alpha \geq 1, \beta \geq 1, \gamma \geq 1,$$

α, β, γ interpret the resources' usage to the network in three dimensions respectively. Swish activation function were used in. Equation (2) define swish function. The EfficientNet architectures B1,B2,B3,B4,B5,B6,B7 as well as other CNN architectures like VGG19,ResNet50,DenseNet169 and Inception V3 are also used in this study.

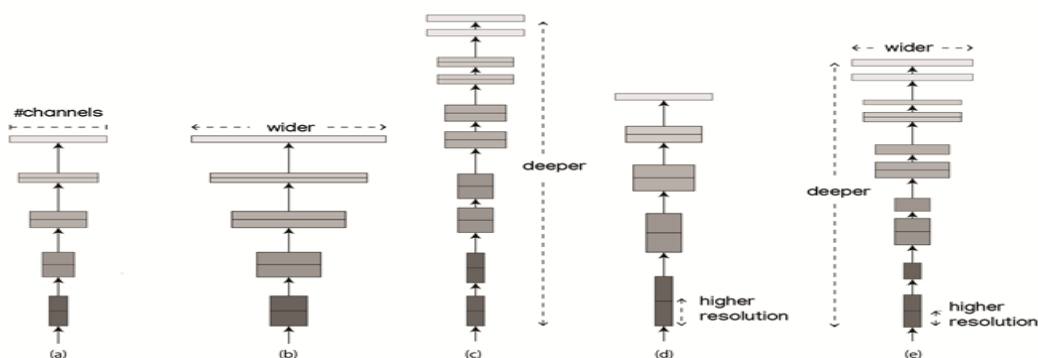


Fig.7. Demonstration of scaling network(a) baseline model(b) Width wise scaling (c) depth wise scaling (d) resolution scaling (e) compound scaling

3.4 Experimental Setting

Fig.4 shows the setup of experiment. The models are implemented as a backend on Keras and TensorFlow framework using Python(3.7.10). Data augmentation technique is applied through various augmenters available in imaug library. EfficientNet models (B1-B7), VGG19, ResNet50, DenseNet169 and Inception V3 were imported using Keras library. Fine tuning of pre-trained CNN models are shown in Fig. 8. Adam optimizer with a learning rate of 10^{-4} , binary cross-entropy function is used as optimizer and to compute the loss of classification respectively. The experiments are implemented in Kaggle kernel .

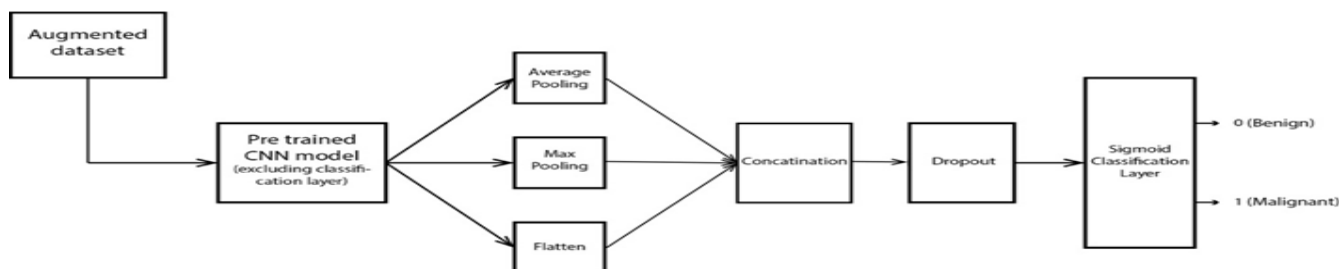


Fig.8. fine tuning of pre-trained architectures of layers with training subset

3.5 Performance Evaluation Methods

The performance of all classification models are decided by computing the confusion matrix for each model. The confusion matrix of each model consisted four values On main diagonal True Negative (TN) and True Positive(TP) in the confusion matrix showed the classification power of each model. Remaining two values represented False positive(FP) and Falsenegative(FN) showed the incorrectness in the classification. Based on these four values the following matrices for every model is computed:

3.5.1 *Accuracy*. It represents the ratio of correctly predicted images with the total images, given by equation (3).

$$\text{Accuracy} = \frac{TP+TN}{TP+TN+FP+FN} \quad (3)$$

3.5.2 *Precision*. It represents the ratio of number of malignant/benign images correctly classified with the total number of predicted malignant/benign images by the model, as given below by equation (4).

$$\text{Precision} = \frac{TP}{TP+FP} \quad (4)$$

3.5.3 *Recall*. It represents the ratio of number of malignant/benign images correctly classified with the total number of actual malignant/benign images, as shown by equation (5).

$$\text{Recall} = \frac{TP}{TP+FN} \quad (5)$$

3.5.4 *F1-score*. It represents the harmonic mean of Precision and Recall and can be used as a metric of classification for imbalanced dataset, as given by equation (6)

$$F1 - \text{score} = \frac{2 \times \text{Precision} \times \text{Recall}}{\text{Precision} + \text{Recall}} \quad (6)$$

4. Results and Discussions

The performance EfficientNet architectures (B1-B7), VGG19, ResNet50, DenseNet169, and InceptionV3 are compared by evaluating the validation accuracy, validation loss, average time taken, number of trainable parameters ,precision value, recall value, and F1-score for each class, average time taken in training ,number of trainable parameters for each model and the result is presented in Table II. It is observed from the table II that EfficientNetB2 and EfficientNetB3 achieve approximately similar results. Among all EfficientNets architectures EfficientNetB6 performs better achieving validation accuracy and validation loss of 96.9% and 0.089 respectively.EfficientNetB4, EfficientNetB5and EfficientNetB7 also showed the satisfactory result for the classification. From the result, it was also observed that the time taken for EfficientNet architectures(in spite of more trainable parameters) achieves the better performance of results than the other pre-trained models with less training time.EfficientNetB3, EfficientNetB4 have trainable parameters between 10M to 20 M produce better accuracy and loss than DenseNet169 with similar range of trainable parameters. So EfficientNet architectures are computationally faster than other CNN models. Although DenseNet169 showed satisfactory results among CNN models other than EfficientNet architectures.

The accuracy graphs, loss graphs, ROC(Receiver Operating Characteristics) are plotted for EfficientNetB4, EfficientNetB5, EfficientNetB6, EfficientNetB7 as well as confusion matrices were also computed. The graphs in Fig.9 showed loss and accuracy curves for four models EfficientNetB4, EfficientNetB5, EfficientNetB6,

EfficientNetB7 with the dataset. For each epoch during training of the model. The curves showed the progress of training and validation accuracy and loss. It is evident from the graphs that the training of all the models are proceeding well. Due to the limitation of computing power only seven epochs are performed for each model.

The graphs in Fig.10. showed the confusion matrices for four models :EfficientNetB4, EfficientNetB5, EfficientNetB6, EfficientNetB7 with the dataset.It is evident from the result that EfficientNet-B6 and EfficientNet-B7 among all four models, were able to classify more accurately with the validation accuracy 96.9% ,96.8 and validation loss 0.089 and 0.0944 respectively .

The graphs in Fig.11. showed the ROC curve for four models :EfficientNet-B4, -B5,-B6, -B7 with the dataset. For each model the curve shows the diagnostic ability with the variation of threshold. In each curve the Area Under Curve(AUC) was also shown. It was seen from the graphs that EfficientNet-B6 and EfficientNet-B4 achieved highest AUC score of 99.5. Data augmentation techniques are also be applied to increase the size of the dataset [33]. The results of the experiment showed that EfficientNet architectures perform better on the used dataset than any previous pre-trained model.

The conventional histopathology methods to diagnose breast cancer is a popular technique to confirm the malignancy by the experts such as pathologists. Being a manual process[8] and lack of trained persons the diagnosis can be delayed for necessary prognosis and treatment and affect mortality. With the advancement of technology pathological techniques are highly improved and became accurate and fast. This has been become possible because of the development of artificial intelligence techniques[16]. Nowadays these methods have been widely applied for medical image analysis[13][34]. Among all deep learning methods specifically, CNN is most popular successful method.[35][21].According to Grand challenge [1], Among all EfficientNet architectures EfficientNetB6 performs better by achieving validation accuracy and validation loss of 96.9% and 0.089 respectively.EfficientNetB4, EfficientNetB4B5 and EfficientNetB4 EfficientNetB7 also show the satisfactory result for the binary classification.

5. Conclusion and Future Work

Among CNN architectures the EfficientNet architecture family performed well on the established image dataset as compared to previous approaches using pre-trained architectures. In the experiment, augmenters are also applied to enhance the semantic information and to resolve the overfitting. Six EfficientNetB1 to EfficientNetB7, VGG19, DenseNet169, ResNet59 and Inception V3 with transfer learning are applied for breast cancer, binary classification in the experiment. The results confirmed that the EfficientNet architectures were able to accurately classify histopathology images into two classes: benign and malignant than other CNN models. Among all EfficientNet architectures EfficientNet-B6 architecture achieved 96.9% validation accuracy, 0.089 validation loss and 99.6 AUC score on the training images. Standard data augmentation techniques were applied for the experiment on publically available dataset. In future advanced data augmentation techniques can be used to increase the generalizability. Further the performance of the models can be checked on real dataset in future. Hybrid CNN models can be developed to improve the performance.

Table. II. comparison of EfficientNet architectures(B1-B7), VGG19,ResNet50,DenseNet169 and Inception V3 for histopathology breast Cancer detection dataset

EfficientNet Model	Validation Accuracy	Validation Loss	Average Time(per Epoch) (seconds)	No of Trainable parameters	Precision for class Benign	Precision for class Malignant	Recall for class Benign	Recall for class Malignant	F1 –score for class Benign	F1 –score for class Malignant
B1	0.963906	0.100241	2042.571	6,527,265	0.97	0.96	0.98	0.95	0.97	0.96
B2	0.967707	0.0938	2035.857	7,716,483	0.97	0.96	0.98	0.95	0.97	0.96
B3	0.96647	0.0938	1972.143	10,713,129	0.97	0.97	0.98	0.96	0.97	0.96
B4	0.968253	0.0917	2176.286	17,568,329	0.97	0.97	0.98	0.96	0.98	0.96
B5	0.96647	0.0929	2326.714	28,363,313	0.96	0.97	0.98	0.95	0.97	0.96
B6	0.969482	0.0898	2442	40,761,049	0.96	0.98	0.99	0.94	0.97	0.96
B7	0.968048	0.0944	2595.286	63,815,121	0.98	0.96	0.97	0.97	0.98	0.96
VGG-19	0.9565	0.1234	2438.714	20,030,017	0.95	0.97	0.98	0.93	0.97	0.95
Dense169	0.9658	0.095	2581.143	12,502,785	0.95	0.98	0.99	0.93	0.97	0.96
ResNet50	0.9613	0.1065	25822		0.96	0.97	0.98	0.95	0.97	0.96
Inception V3	0.9466	0.1418	2247.571	21,772,449	0.93	0.97	0.98	0.9	0.96	0.93

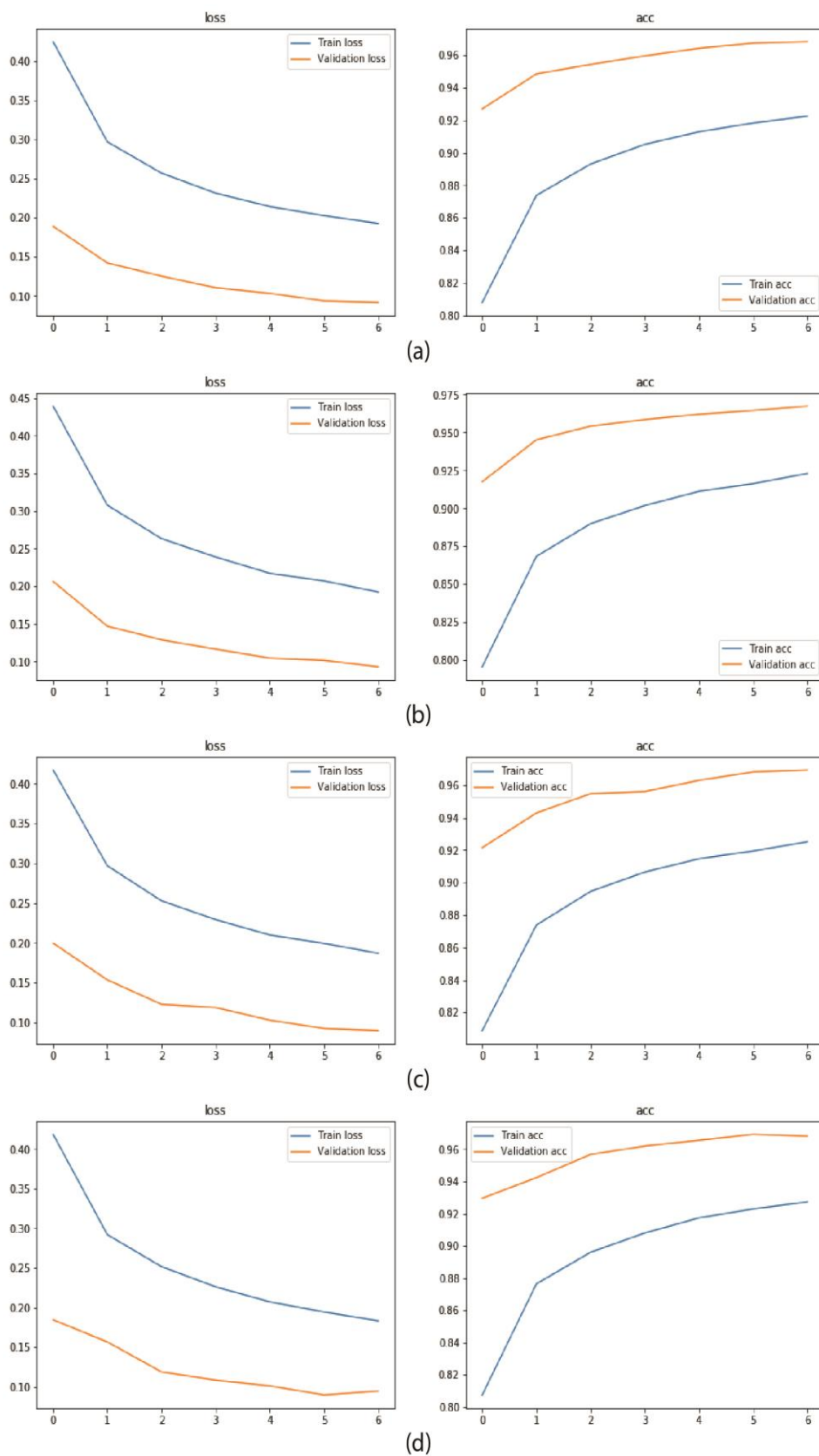


Fig. 9. Loss and accuracy graphs: (a) EfficientNet-B4 loss and accuracy graph; (b) EfficientNet-B5 loss and accuracy graph; (c) EfficientNet-B6 loss and accuracy graph; (d) EfficientNet-B7 loss and accuracy graph

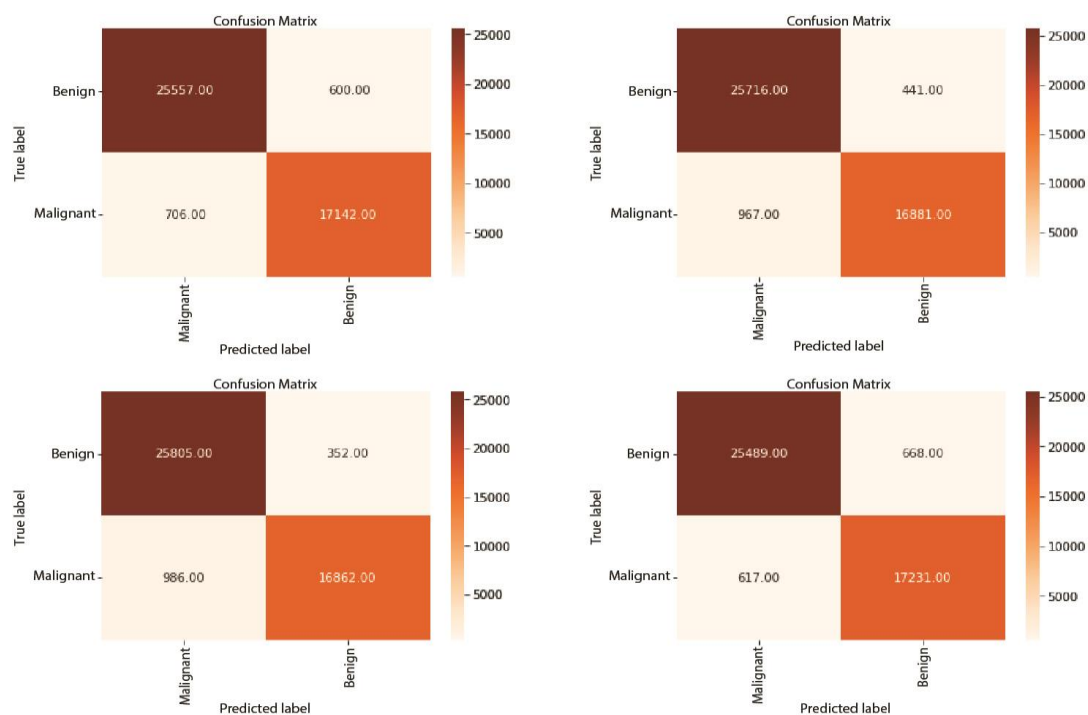


Fig.10.confusion Matrix: (a) EfficientNet-B4 ROC curve graph; (b) EfficientNet-B5 ROC curve graph

(c) EfficientNet-B6 ROC curve graph (d) EfficientNet-B7

References

- [1] C. Munien and S. Viriri, "Classification of Hematoxylin and Eosin-Stained Breast Cancer Histology Microscopy Images Using Transfer Learning with EfficientNets," *Comput. Intell. Neurosci.*, vol. 2021, 2021, doi: 10.1155/2021/5580914.
- [2] H. Sung *et al.*, "Global Cancer Statistics 2020: GLOBOCAN Estimates of Incidence and Mortality Worldwide for 36 Cancers in 185 Countries," *CA. Cancer J. Clin.*, vol. 71, no. 3, pp. 209–249, May 2021, doi: 10.3322/caac.21660.
- [3] "Cancer cases in India estimated to be 13.9 lakh in 2020, may rise to 15.7 lakh by 2025: Report | India News - Times of India." <https://timesofindia.indiatimes.com/india/cancer-cases-in-india-estimated-to-be-13-9-lakh-in-2020-may-rise-to-15-7-lakh-by-2025-report/articleshow/77628680.cms>.
- [4] "Report of National Cancer Registry Programme," 2012.
- [5] M. I. Nounou, F. Elamrawy, N. Ahmed, K. Abdelraouf, S. Goda, and H. Syed-Sha-Qhattal, "Breast cancer: Conventional diagnosis and treatment modalities and recent patents and technologies supplementary issue: Targeted therapies in breast cancer treatment," *Breast Cancer Basic Clin. Res.*, vol. 9, pp. 17–34, 2015, doi: 10.4137/BCBCR.S29420.
- [6] "Clinical Edge Journal Scan Commentary: Breast Cancer July 2021 | MDedge Hematology and Oncology." <https://www.mdedge.com/hematology-oncology/article/241898/breast-cancer/clinical-edge-journal-scan-commentary-breast-cancer> (accessed Sep. 07, 2021).
- [7] T. M. Allweis, N. Hermann, R. Berenstein-Molho, and M. Guindy, "Personalized Screening for Breast Cancer: Rationale, Present Practices, and Future Directions," *Ann. Surg. Oncol.* 2021 288, vol. 28, no. 8, pp. 4306–4317, Jan. 2021, doi: 10.1245/S10434-020-09426-1.
- [8] M. I. Sarker, H. Kim, D. Tarasov, and D. Akhmetzanov, "Inception Architecture and Residual Connections in Classification of Breast Cancer Histology Images Inception Architecture and Residual Connections in Classification of Breast Cancer Histology Images," no. December 2019, 2020.
- [9] H. Harvey *et al.*, "The Role of Deep Learning in Breast Screening," *Curr. Breast Cancer Rep.*, vol. 11, no. 1, pp. 17–22, 2019, doi: 10.1007/s12609-019-0301-7.
- [10] A. Al Nahid and Y. Kong, "Involvement of Machine Learning for Breast Cancer Image Classification: A Survey," *Computational and Mathematical Methods in Medicine*, vol. 2017. Hindawi Limited, 2017, doi:

- 10.1155/2017/3781951.
- [11] S. Sharma and S. Deshpande, "Breast Cancer Classification Using Machine Learning Algorithms," *Lect. Notes Networks Syst.*, vol. 141, no. 14, pp. 571–578, 2021, doi: 10.1007/978-981-15-7106-0_56.
- [12] A.-A. Nahid and Y. Kong, "Involvement of Machine Learning for Breast Cancer Image Classification: A Survey," 2017, doi: 10.1155/2017/3781951.
- [13] N. Fatima, L. Liu, S. Hong, and H. Ahmed, "Prediction of Breast Cancer, Comparative Review of Machine Learning Techniques, and Their Analysis," *IEEE Access*, vol. 8, pp. 150360–150376, 2020, doi: 10.1109/access.2020.3016715.
- [14] H. Asri, H. Mousannif, H. Al Moatassime, and T. Noel, "Using Machine Learning Algorithms for Breast Cancer Risk Prediction and Diagnosis," *Procedia Comput. Sci.*, vol. 83, no. Fams, pp. 1064–1069, 2016, doi: 10.1016/j.procs.2016.04.224.
- [15] G. B.M, S. C.P, and S. T, "Breast Cancer Diagnosis Using Machine Learning Algorithms - A Survey," *Int. J. Distrib. Parallel Syst.*, vol. 4, no. 3, pp. 105–112, 2013, doi: 10.5121/ijdps.2013.4309.
- [16] S. Bharati, P. Podder, and M. R. H. Mondal, "Artificial Neural Network Based Breast Cancer Screening: A Comprehensive Review," pp. 1–13.
- [17] D. Jarrett, E. Stride, K. Vallis, and M. J. Gooding, "Applications and limitations of machine learning in radiation oncology," <https://doi.org/10.1259/bjr.20190001>, vol. 92, no. 1100, Jun. 2019, doi: 10.1259/BJR.20190001.
- [18] G. Litjens *et al.*, "A survey on deep learning in medical image analysis," *Med. Image Anal.*, vol. 42, no. 1995, pp. 60–88, 2017, doi: 10.1016/j.media.2017.07.005.
- [19] X. Li, X. Shen, Y. Zhou, X. Wang, and T. Q. Li, "Classification of breast cancer histopathological images using interleaved DenseNet with SENet (IDSNet)," *PLoS One*, vol. 15, no. 5, pp. 1–13, 2020, doi: 10.1371/journal.pone.0232127.
- [20] A. Riasatian, M. Rasoolijaberi, M. Babaei, and H. R. Tizhoosh, "A Comparative Study of U-Net Topologies for Background Removal in Histopathology Images," Jun. 2020, Accessed: Aug. 11, 2020. [Online]. Available: <http://arxiv.org/abs/2006.06531>.
- [21] J. Wang, Q. Liu, H. Xie, Z. Yang, and H. Zhou, "Boosted EfficientNet: Detection of Lymph Node Metastases in Breast Cancer Using Convolutional Neural Network," Oct. 2020, Accessed: Jan. 09, 2021. [Online]. Available: <http://arxiv.org/abs/2010.05027>.
- [22] Y. Sun, F. A. Binti Hamzah, and B. Mochizuki, "Optimized Light-Weight Convolutional Neural Networks for Histopathologic Cancer Detection," in *LifeTech 2020 - 2020 IEEE 2nd Global Conference on Life Sciences and Technologies*, Mar. 2020, pp. 11–14, doi: 10.1109/LifeTech48969.2020.1570619224.
- [23] M. M. Khapra, "CS7015 (Deep Learning) : Lecture 8."
- [24] C. Shorten and T. M. Khoshgoftaar, "A survey on Image Data Augmentation for Deep Learning," *J. Big Data*, vol. 6, no. 1, p. 60, Dec. 2019, doi: 10.1186/s40537-019-0197-0.
- [25] O. C. Baltatu *et al.*, "Article 629134 W and Nicolaou S (2021) The Effectiveness of Image Augmentation in Deep Learning Networks for Detecting COVID-19: A Geometric Transformation Perspective," *Front. Med*, vol. 8, p. 629134, 2021, doi: 10.3389/fmed.2021.629134.
- [26] E. K. Kim, H. Lee, J. Y. Kim, and S. Kim, "Data Augmentation Method by Applying Color Perturbation of Inverse PSNR and Geometric Transformations for Object Recognition Based on Deep Learning," *Appl. Sci.*, vol. 10, no. 11, p. 3755, May 2020, doi: 10.3390/app10113755.
- [27] "DATA AUGMENTATION IN TRAINING CNNs: INJECTING NOISE TO IMAGES."
- [28] "Advanced Data Augmentation Strategies | by Connor Shorten | Towards Data Science." <https://towardsdatascience.com/advanced-data-augmentation-strategies-383226cd11ba> (accessed Mar. 05, 2021).
- [29] "Histopathologic Cancer Detection | Kaggle." <https://www.kaggle.com/c/histopathologic-cancer-detection> (accessed Mar. 08, 2021).
- [30] "imgaug — imgaug 0.4.0 documentation." <https://imgaug.readthedocs.io/en/latest/> (accessed Jul. 29, 2021).
- [31] "Overview of Augmenters —0.4.0 documentation" https://imgaug.readthedocs.io/en/latest/source/overview_of_augmenters.html
- [32] M. Tan and Q. V. Le, "EfficientNet: Rethinking Model Scaling for Convolutional Neural Networks," *36th Int. Conf. Mach. Learn. ICML 2019*, vol. 2019-June, pp. 10691–10700, May 2019, Accessed: Aug. 09, 2020. [Online]. Available: <http://arxiv.org/abs/1905.11946>.
- [33] Q. Zheng, M. Yang, X. Tian, N. Jiang, and D. Wang, "A full stage data augmentation method in deep convolutional neural network for natural image classification," *Discret. Dyn. Nat. Soc.*, vol. 2020, 2020, doi: 10.1155/2020/4706576.
- [34] T. D. Truong and H. T. T. Pham, "Breast Cancer Histopathological Image Classification Utilizing Convolutional Neural Network," *IFMBE Proc.*, vol. 69, pp. 531–536, 2020, doi: 10.1007/978-981-13-5859-3_92.
- [35] S. C. Kosaraju, J. Hao, H. M. Koh, and M. Kang, "Deep-Hipo: Multi-scale receptive field deep learning for histopathological image analysis," *Methods*, vol. 179, pp. 3–13, Jul. 2020, doi: 10.1016/j.ymeth.2020.05.012